Engineering Structures 82 (2015) 151–167

Contents lists available at ScienceDirect

Engineering Structures

journal homepage: www.elsevier.com/locate/engstruct

Correlation between ground motion intensity measures and seismic damage of 3D R/C buildings

Konstantinos Kostinakis [a,*], Asimina Athanatopoulou [a], Konstantinos Morfidis [b]

[a] Department of Civil Engineering, Aristotle University of Thessaloniki, Aristotle University Campus, 54124 Thessaloniki, Greece
[b] Institute of Engineering Seismology and Earthquake Engineering (ITSAK-EPPO), 5 Ag. Georgiou Str., 55535 Thessaloniki, Greece

ARTICLE INFO

Article history:
Received 1 November 2013
Revised 28 June 2014
Accepted 20 October 2014

Keywords:
Reinforced concrete
Damage indices
Time history analysis
Seismic excitation angle
Seismic damage
Ground motion IMs

ABSTRACT

The present paper investigates the correlation between a large number of widely used ground motion intensity measures (IMs) and the corresponding damage to medium-rise 3D, R/C buildings. To accomplish this purpose the seismic performance of two symmetric and two asymmetric in plan 5-storey buildings subjected to 64 bidirectional earthquake ground motions are determined. Structural performance is expressed in terms of the maximum and the average interstorey drift as well as the overall structural damage index and it is determined for many angles of seismic incidence. For each individual pair of accelerograms and each seismic input angle the values of the aforementioned seismic damage measures are determined. Then, the correlation between the damage measures and the IMs is evaluated. The results reveal that the spectral acceleration at the fundamental period of the structure shows the strongest correlation with the maximum and average interstorey drifts, followed by the velocity related seismic IMs. Moreover, the vast majority of the examined ground motion IMs are proved to be inadequate to predict the overall structural damage index of frame-wall (dual) systems.

1. Introduction

An important area of research in seismic risk analysis is the evaluation of expected seismic damage of structures under a specific earthquake ground motion. To estimate the structural damage potential of an earthquake it is necessary to introduce two intermediate variables, one describing the structural performance and the other describing the ground motion intensity. A successful correlation of the aforementioned variables ensures more accurate evaluation of seismic performance and a sufficient reduction in the variability of structural response prediction. Consequently, the identification of an optimal intensity measure, which sufficiently correlates with an appropriate engineering demand parameter, is of great importance. The expected seismic performance is usually described by displacement demands, such as maximum interstorey drift, as well as deformation demands in the structural elements. On the other hand, many ground motion intensity measures (IMs) have been proposed as efficient predictors of the structural response level.

Elenas [1,2] and Elenas and Meskouris [3] studied the interdependency between several seismic acceleration parameters and the damage state of a 6-storey [1] and an 8-storey [2,3] planar R/C frame structure. The damage response parameters that were evaluated were the maximum horizontal displacement at the top of the building [1], the curvature ductility demand at the base of a column [1], the Park and Ang overall structural damage index [2,3], the maximum softening index after DiPasquale/Cakmak [2], the maximum interstorey drift [3] and the maximum floor acceleration [3]. They observed that for the structures under consideration spectral and energy related seismic intensity measures correlate well with seismic damage.

Liao et al. [4], based on limited analyses of planar frames (5-storey and 12-storey R/C buildings), demonstrated that three parameters of the near-fault earthquake records, i.e. the PGV/PGA ratio, the spectral velocity and the input energy, are well correlated with the maximum storey drift of the structures. Another study carried out by Riddell [5] examined the efficiency of 23 ground motion intensity measures to characterize the maximum inelastic displacement and the dissipated energy of simple SDOF systems representative of the three characteristic spectral regions. The results showed that none of the ground IMs was satisfactory over the entire frequency range. The same conclusion was reached by San et al. [6], who studied the structural damage of a typical planar 5-storey R/C frame subjected to ground motions from Kocaeli

* Corresponding author at: Pasalidi 19, Kato Toumpa, 54453 Thessaloniki, Greece. Tel.: +30 6945349502.
E-mail addresses: kkostina@civil.auth.gr (K. Kostinakis), minak@civil.auth.gr (A. Athanatopoulou), kmorfidis@itsak.gr (K. Morfidis).

http://dx.doi.org/10.1016/j.engstruct.2014.10.035
0141-0296/

(Turkey) earthquake. The seismic damage was expressed in terms of the maximum interstorey drift ratio, as well as of the overall structural damage index after Park and Ang. Yakut and Yilmaz [7] investigated the correlation between maximum interstorey drift demand of 16 planar R/C frame structures and a number of widely used ground motion intensity measures. The results of this study demonstrated that spectral intensity parameters have the strongest correlation with the maximum interstorey drift.

In a similar investigation, Masi et al. [8] correlated various measures of seismic intensity with the maximum interstorey drift of typical 4-storey planar R/C frames taking into account the influence of the masonry infills. They found that the Housner intensity is the IM that best correlates with the maximum interstorey drift for the strong ground motions used in their study. In another study (Ye et al. [9]), several earthquake intensity measures published in the literature were evaluated through correlation analysis using SDOF as well MDOF structural systems (lumped mass shear storey models and planar shear wall structures). Their analyses revealed that Peak Ground Velocity shows good correlation with the structural damage except for very stiff systems with high frequency.

It must be noted that all the above investigations were restricted to planar R/C frames, thus taking into account only one component of the strong motion records. Modern seismic codes [10–14] suggest that structures shall be designed for the two horizontal translational components of ground motion (in the majority of buildings the vertical component may be neglected). In order to examine the adequacy of seismic intensity measures to describe the structural response of R/C buildings under bidirectional strong motions, Cantagallo et al. [15] investigated correlations between maximum interstorey drift demand of nine simple 3D structures and a number of IMs. They showed that spectral and energy IMs provide in general good correlation with the maximum interstorey drift. Besides, Lucchini et al. [16] studied the efficiency of 5 IMs in correlating with the maximum interstorey drift and the peak roof drift ratio (i.e. the ratio of the peak lateral roof displacement to the building height). In their study they analyzed the so-called "Spear building" under 120 pairs of recordings. They concluded that the spectral acceleration corresponding to the fundamental period of the structure shows a rather weak correlation with the above mentioned engineering demand parameters. In these two studies the two horizontal components of the earthquake records were applied along the structural axes of the buildings, thus the uncertainty introduced in the structural response by the seismic excitation angle is ignored.

As it has been shown by many researchers, even for quite simple buildings, the angle of seismic incidence can radically alter the analysis results in terms of the elastic response and design of structures, e.g. [17–19], as well as of the inelastic response and damage level, e.g. [20–24]. In a preliminary study, Fontara et al. [25] examined the interrelationship between commonly used seismic intensity measures and the Park and Ang overall structural damage index of an asymmetric 3D single-storey R/C building taking into account several incident angles. The research revealed that the intensity measures which have strong correlation to the overall damage index, whether the latter is caused by recorded, uncorrelated or completely correlated pairs of accelerograms, are the Arias intensity and the cumulative absolute velocity.

From the abovementioned studies, it is obvious that several researchers have investigated a large number of earthquake IMs. Nevertheless, no general consensus exists regarding the best predictor of the seismic response, since it depends on the structural system and the ground motions used. Moreover, the up-to-date research concerns mainly planar frames. Three studies deal with 3D structures under bidirectional excitation. The two of them [15,16] do not account for the impact of the seismic orientation while the third one [25], which accounts for seismic orientation, deals with only one single storey structure.

The objective of the present paper is to investigate the correlation between a large number of widely used ground motion IMs and the seismic response of medium-rise, 3D, R/C buildings considering different orientations of the earthquake ground motion. For this purpose, four 3D, R/C buildings are analyzed for 64 bidirectional strong motions using Nonlinear Time History Analysis (NTHA). In order to account for the influence of the incident angle on the structural response, the two horizontal accelerograms of each ground motion are applied along horizontal orthogonal axes forming an angle $\theta = 0°, 5°, 10°, \ldots, 355°$ with the structural axes. For the evaluation of the inelastic structural behavior of each building the overall structural damage index, as well as the maximum and average interstorey drift, are computed. Then, the aforementioned structural damage parameters are correlated with the examined IMs. Among the ground motion intensity measures investigated, the spectral acceleration at the fundamental period of the structure has the strongest correlation with damage, followed by the velocity related IMs. Moreover, the overall structural damage index shows medium or poor correlation with the majority of the IMs.

2. Ground motions

A suite of 64 pairs of horizontal bidirectional earthquake excitations obtained from the PEER [26] and the European [27] strong motion databases are used as input ground motion for the analyses. The seismic excitations, which have been chosen from worldwide well known sites with strong seismic activity, are recorded on Soil Type C according to EC8 [11] and have magnitudes (M_s) between 5.5 and 7.8. The ground motion set employed was intended to cover a variety of conditions regarding tectonic environment, modified Mercalli intensity and closest distance to fault rapture, thus representing a wide range of intensities and frequency content. Furthermore, note that the duration of the seismic records ranges between 11.2 s. and 149.1 s. Another aspect considered on the selection of the seismic excitations is that they provide a wide spectrum of structural damage, from negligible to severe, to the buildings investigated in the present study.

The recorded horizontal accelerograms of each ground motion were transformed to the corresponding uncorrelated ones rotating them about the vertical axis by the angle θ_o (Eq. (1)) [28]. Then, the pairs of the uncorrelated accelerograms have been used as seismic input for the analyses of the structures, as ASCE 41-06 [10] proposes. The characteristics of the input ground motions are shown in Table 1 along with the correlation factor of the recorded components ρ [28], which is given by Eq. (1):

$$\rho = \frac{\sigma_{xy}}{(\sigma_{xx}\cdot\sigma_{yy})^{1/2}}, \quad \tan 2\theta_o = \frac{2\sigma_{xy}}{\sigma_{xx}-\sigma_{yy}}$$
$$\text{with } \sigma_{ij} = \frac{1}{t_{tot}}\cdot\left(\int_0^{t_{tot}} \alpha_i(t)\cdot\alpha_j(t)dt\right) \quad i = x, y \tag{1}$$

where $\alpha_x(t)$ and $\alpha_y(t)$ are the recorded ground accelerations along two horizontal directions of the ground motion; σ_{xx}, σ_{yy} are the quadratic intensities of $\alpha_x(t)$ and $\alpha_y(t)$ respectively; σ_{xy} is the corresponding cross-term; and t_{tot} is the duration of the motion.

We note that we have used unscaled accelerograms for the nonlinear dynamic analyses, because scaling of the earthquake records would give a falsified value of the interdependency between the seismic parameters and the structural damage. The vast majority of the published studies dealing with the correlation have also used unscaled accelerograms (see for example [3,7,15]).

Table 1
Ground motion recorded on Soil Type C according to EC8 [11].

No.	Date	Earthquake name	Magnitude (M_s)	Station name	Closest distance (km)	Component (deg)	PGA (g)	Duration (s)	Corr. factor (ρ)
1	15/10/1979	Imperial Valley	6.9	Compuertas	32.6	015	0.186	36.0	0.16
						285	0.147		
2	17/8/1999	Kocaeli, Turkey	7.8	Atakoy	67.5	000	0.105	133.1	−0.04
						090	0.164		
3	17/8/1999	Kocaeli, Turkey	7.8	Cekmece	76.1	000	0.179	149.1	0.12
						090	0.133		
4	28/6/1992	Landers	7.4	Coachella Canal	55.7	000	0.104	60.0	0.19
						090	0.109		
5	18/10/1989	Loma Prieta	7.1	Halls Valley	31.6	090	0.134	40.0	0.04
						180	0.103		
6	18/10/1989	Loma Prieta	7.1	Agnews State Hospital	28.2	090	0.172	40.0	0.15
						180	0.159		
7	18/10/1989	Loma Prieta	7.1	Gilroy Array #7	24.2	090	0.226	40.0	−0.30
						180	0.323		
8	24/4/1984	Morgan Hill	6.1	Hollister City Hall	32.5	001	0.071	28.3	−0.15
						271	0.071		
9	17/1/1994	Northridge	6.7	Downey – Birchdale	40.7	090	0.165	35.0	0.24
						180	0.171		
10	17/1/1994	Northridge	6.7	Glendale – Las Palmas	25.4	177	0.357	30.0	−0.05
						267	0.206		
11	2/5/1983	Coalinga	6.5	Parkfield – Cholame 5W	47.3	270	0.147	40.0	−0.10
						360	0.131		
12	2/5/1983	Coalinga	6.5	Parkfield – Cholame 8W	50.7	000	0.098	32.0	−0.28
						270	0.100		
13	1/10/1987	Whittier Narrows	5.7	Bell Gardens – Jaboneria	9.8	207	0.219	34.3	−0.02
						297	0.212		
14	1/10/1987	Whittier Narrows	5.7	El Monte – Fairview Av	9.8	000	0.120	28.3	0.23
						270	0.228		
15	1/10/1987	Whittier Narrows	5.7	Santa Fe Springs – E Joslin	10.8	048	0.426	37.8	−0.08
						318	0.443		
16	19/5/1940	Imperial Valley	7.2	El Centro Array #9	8.3	180	0.313	40.0	−0.13
						270	0.215		
17	28/6/1966	Parkfield		Cholame #5	5.3	085	0.442	43.9	−0.15
						355	0.367		
18	20/9/1999	Chi–Chi, Taiwan	7.6	TCU	2.94	N	0.251	49.0	−0.33
						W	0.202		
19	20/9/1999	Chi–Chi, Taiwan	7.6	TCU	4.01	N	0.162	90.0	−0.10
						W	0.134		
20	20/9/1999	Chi–Chi, Taiwan	7.6	TCU	4.5	N	0.251	90.0	−0.08
						W	0.293		
21	18/10/1989	Loma Prieta	7.1	Gilroy Array #3	14.4	000	0.555	39.9	0.05
						090	0.367		
22	1/10/1987	Whittier Narrows	5.7	LA – Fletcher Dr	14.4	144	0.171	32.0	−0.04
						234	0.231		
23	7/12/1988	Spitak	6.7	Gukasian	20	E–W	0.183	23.0	−0.05
						N–S	0.183		
24	20/6/1990	Manjil (Iran)	7.4	Abhar	75	N57E	0.132	29.5	−0.33
						N33W	0.209		
25	20/6/1990	Manjil (Iran)	7.4	Rudsar	61	N40E	0.097	52.2	−0.02
						N50W	0.086		
26	17/8/1999	Izmit (Turkey)	7.6	Iznik-Karayollari Sefligi Muracaati	29	W–E	0.129	53.1	0.02
						S–N	0.091		
27	17/8/1999	Izmit (Turkey)	7.6	Istanbul-Zeytinburnu	80	E–W	0.114	100.0	0.05
						N–S	0.110		
28	11/9/1976	Friuli (Italy)	5.5	Buia	7	E–W	0.105	20.3	0.04
						N–S	0.230		
29	15/9/1976	Friuli (Italy)	6	Buia	9	E–W	0.095	26.4	−0.07
						N–S	0.109		
30	24/2/1981	Aktion (Greece)	6.6	Korinthos-OTE Building	10	N30	0.230	41.9	−0.28
						N120	0.310		
31	7/12/1988	Spitak		Gukasian	10	E–W	0.103	21.4	0.11
						N–S	0.147		
32	26/9/1997	Umbria Marche (Italy)	6	Colfiorito	5	N–S	0.199	48.5	−0.11
						W–E	0.223		
33	12/11/1999	Duzce Turkey)	7.2	LDEO Station No. C1062 FI	14	E–W	0.254	42.3	0.13
						N–S	0.114		
34	28/6/1992	Landers	7.4	Yermo Fire Station	24.9	270	0.245	44.0	−0.20
						360	0.152		
35	27/1/1980	Livermore	5.5	San Ramon – Eastman Kodak	17.6	180	0.301	21.7	−0.23
						270	0.097		
36	18/10/1989	Loma Prieta	7.1	Gilroy Array #4	16.1	000	0.417	40.0	0.06
						090	0.212		

(*continued on next page*)

Table 1 (*continued*)

No.	Date	Earthquake name	Magnitude (M_s)	Station name	Closest distance (km)	Component (deg)	PGA (g)	Duration (s)	Corr. factor (ρ)
37	18/10/1989	Loma Prieta	7.1	Oakland – Title & Trust	77.4	180	0.195	40.0	0.03
						270	0.244		
38	18/10/1989	Loma Prieta	7.1	Sunnyvale – Colton Ave.	28.2	270	0.207	39.3	−0.10
						360	0.209		
39	17/1/1994	Northridge	6.7	Downey – Co Maint Bldg	47.6	090	0.158	40.0	−0.03
						360	0.230		
40	17/1/1994	Northridge	6.7	LA – Fletcher Dr	29.5	144	0.162	30.0	0.17
						234	0.240		
41	17/1/1994	Northridge	6.7	LA – N Faring Rd	23.9	000	0.273	30.0	−0.18
						090	0.242		
42	17/1/1994	Northridge	6.7	LA – S Grand Ave	36.9	090	0.290	30.0	−0.07
						180	0.264		
43	17/1/1994	Northridge	6.7	La Habra – Briarcliff	61.6	000	0.109	35.0	0.12
						090	0.206		
44	17/1/1994	Northridge	6.7	Manhattan Beach – Manhattan	42	000	0.201	35.0	0.07
						090	0.128		
45	17/1/1994	Northridge	6.7	Pasadena – N Sierra Madre	39.2	180	0.245	19.9	0.12
						270	0.174		
46	9/2/1971	San Fernando	6.6	LA – Hollywood Stor Lot	21.2	090	0.210	28.0	0.18
						180	0.174		
47	24/11/1987	Superstitn Hills	6.6	Calipatria Fire Station	28.3	225	0.180	22.1	0.17
						315	0.247		
48	1/10/1987	Whittier Narrows	5.7	Glendale – Las Palmas	19	177	0.296	31.5	0.04
						267	0.166		
49	1/10/1987	Whittier Narrows	5.7	Lakewood – Del Amo Blvd	20.9	000	0.277	29.8	0.15
						090	0.178		
50	1/10/1987	Whittier Narrows	5.7	Studio City – Coldwater Can	28.7	092	0.177	32.4	−0.11
						182	0.231		
51	8/7/1986	N. Palm Springs	6	Palm Springs Airport	16.6	000	0.158	30.0	0.14
						090	0.187		
52	17/1/1994	Northridge	6.7	LA – Pico & Sentous	32.7	090	0.103	40.0	−0.05
						180	0.186		
53	17/1/1994	Northridge	6.7	Leona Valley #6	38.5	090	0.178	32.0	−0.02
						360	0.131		
54	24/11/1987	Superstitn Hills	6.6	Plaster City	21	045	0.121	22.2	0.27
						135	0.186		
55	24/1/1980	Livermore	5.5	San Ramon – Eastman Kodak	17.6	180	0.154	21.0	−0.35
						270	0.076		
56	18/10/1989	Loma Prieta	7.1	APEEL 2E Hayward Muir Sch	57.4	000	0.171	40.0	−0.04
						090	0.139		
57	17/1/1994	Northridge	6.7	Elizabeth Lake	37.2	090	0.155	40.0	−0.18
						180	0.109		
58	15/10/1979	Imperial Valley	6.9	Aeropuerto Mexicali	8.5	045	0.327	11.2	−0.07
						315	0.260		
59	15/10/1979	Imperial Valley	6.9	Calexico Fire Station	10.6	225	0.275	37.8	0.04
						315	0.202		
60	15/10/1979	Imperial Valley	6.9	El Centro Array #10	8.6	050	0.171	37.0	0.13
						320	0.224		
61	24/11/1987	Superstitn Hills	6.6	Westmorland Fire Sta	13.3	090	0.172	40.0	0.08
						180	0.211		
62	24/4/1984	Morgan Hill	6.1	Gilroy Array #4	12.8	270	0.224.	40.0	−0.36
						360	0.348		
63	15/10/1979	Imperial Valley	6.9	El Centro Array #11	12.6	140	0.364	39.0	0.34
						230	0.380		
64	24/4/1984	Morgan Hill	6.1	Halls Valley	3.4	150	0.156	40.0	0.16
						240	0.312		

3. Ground motion intensity measures

In order to define the intensity of the earthquake ground motion a large number of seismic intensity measures cited in the literature are considered in the present study. The definition as well as a discussion on the employment of each IM is presented in Kramer [29]. It must be noticed that many of the examined IMs have been widely used for correlation studies between seismic intensity and the damage state of planar structures [2–9,15].

In particular, the following ground motions intensity measures are numerically assessed:

1. IMs determined from the time histories of the records.
   - 1.1. *Peak Ground Acceleration:* PGA = $\max|a(t)|$.
   - 1.2. *Peak Ground Velocity:* PGV = $\max|v(t)|$.
   - 1.3. *Peak Ground Displacement:* PGD = $\max|d(t)|$.
   - 1.4. *Peak velocity/acceleration ratio:* $\frac{PGV}{PGA}$.
   - 1.5. *Sustained Maximum Acceleration (SMA)* defined as the 3rd largest peak in the acceleration time history.
   - 1.6. *Sustained Maximum Velocity (SMV)* defined as the 3rd largest peak in the velocity time history.
   - 1.7. *Effective Design Acceleration (EDA)* corresponds to the peak acceleration value that remains after filtering out accelerations above 9 Hz.
   - 1.8. *Root-Mean-Square (rms) of acceleration:* $a_{rms} = \sqrt{\frac{1}{t_{tot}}\int_0^{t_{tot}} a(t)^2 dt}$.
   - 1.9. *Root-Mean-Square (rms) of velocity:* $v_{rms} = \sqrt{\frac{1}{t_{tot}}\int_0^{t_{tot}} v(t)^2 dt}$.

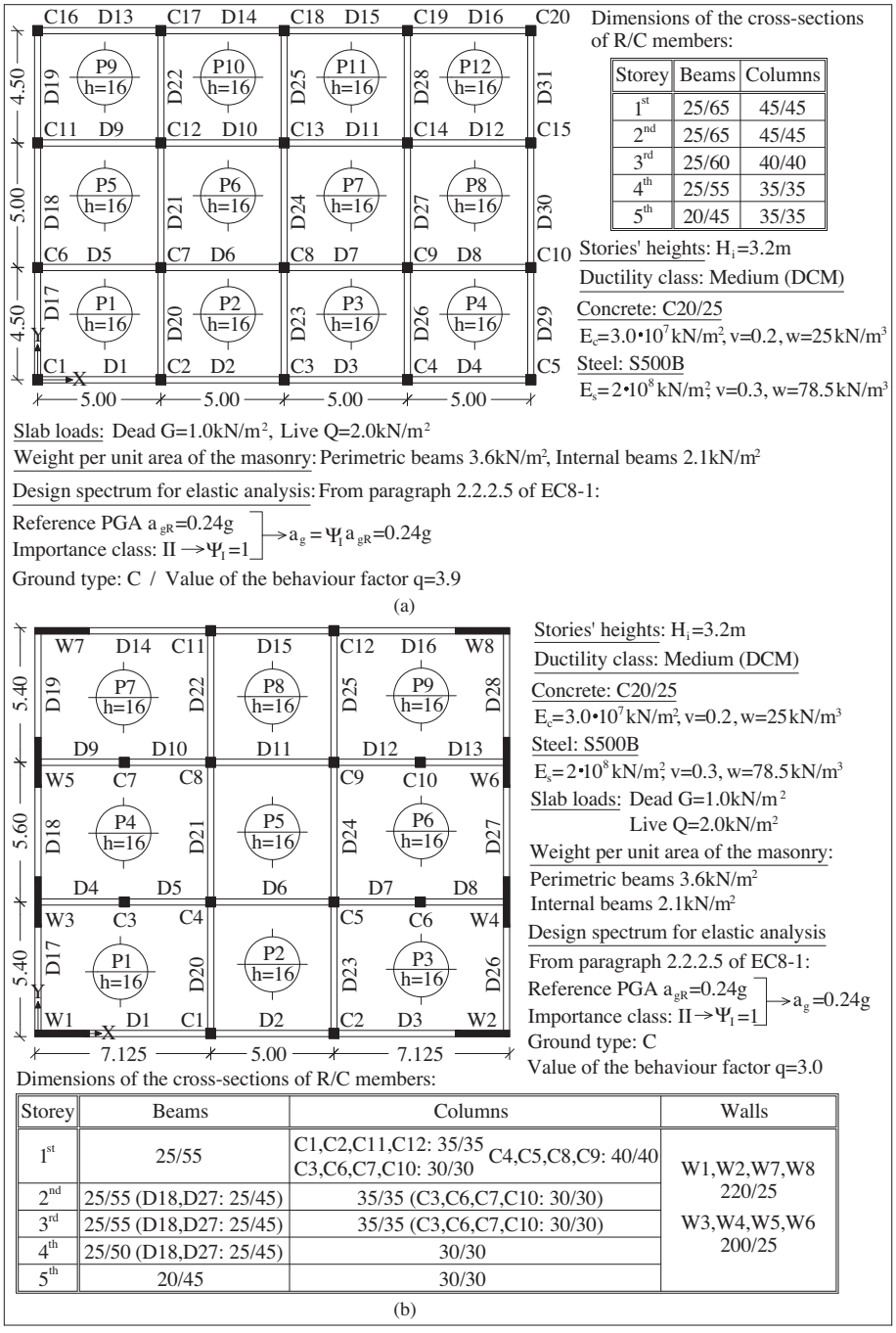

Fig. 1. 5-storey symmetric buildings: (a) SFS and (b) SWS. Plan views, geometrical and design parameters.

1.10. *Root-Mean-Square (rms) of displacement:* $d_{\text{rms}} = \sqrt{\frac{1}{t_{\text{tot}}}\int_0^{t_{\text{tot}}} d(t)^2 dt}$.

1.11. *Arias intensity:* $I_a = \frac{\pi}{2g}\int_0^{t_{\text{tot}}} a(t)^2 dt$.

1.12. *Characteristic intensity:* $I_c = (a_{\text{rms}})^{2/3}\sqrt{t_{\text{tot}}}$.

1.13. *Specific Energy Density:* $\text{SED} = \int_0^{t_{\text{tot}}} v(t)^2 dt$.

1.14. *Cumulative Absolute Velocity:* $\text{CAV} = \int_0^{t_{\text{tot}}} |a(t)| dt$.

2. IMs determined from the response spectra of the records.

2.1. *Spectral acceleration at the fundamental period of the structure T_1:* $S_a(T_1)$.

2.2. *Acceleration Spectrum Intensity:* $\text{ASI} = \int_{0.1}^{0.5} S_a(\xi = 0.05, T) dT$.

2.3. *Velocity Spectrum Intensity:* $\text{VSI} = \int_{0.1}^{2.5} S_v(\xi = 0.05, T) dT$.

2.4. *Housner Intensity:* $\text{HI} = \int_{0.1}^{2.5} \text{PS}_v(\xi = 0.05, T) dT$.

2.5. *Effective Peak Acceleration:* $\text{EPA} = \frac{\text{mean}\left(S_a^{0.1-0.5}(\xi=0.05)\right)}{2.5}$.

where $a(t)$, $v(t)$ and $d(t)$: acceleration, velocity and displacement time history respectively; t_{tot}: total duration of ground motion; ξ: damping ratio; S_a. S_v: spectral acceleration and velocity respectively; PS_v: spectral pseudovelocity.

The aforementioned IMs are determined for each one of the two components of the 64 bidirectional strong motions. However, in order to study the correlation of the IMs with the structural damage of the buildings, it was necessary to represent the intensity parameters corresponding to the two horizontal components by a single value. To achieve this, the following relations, which are

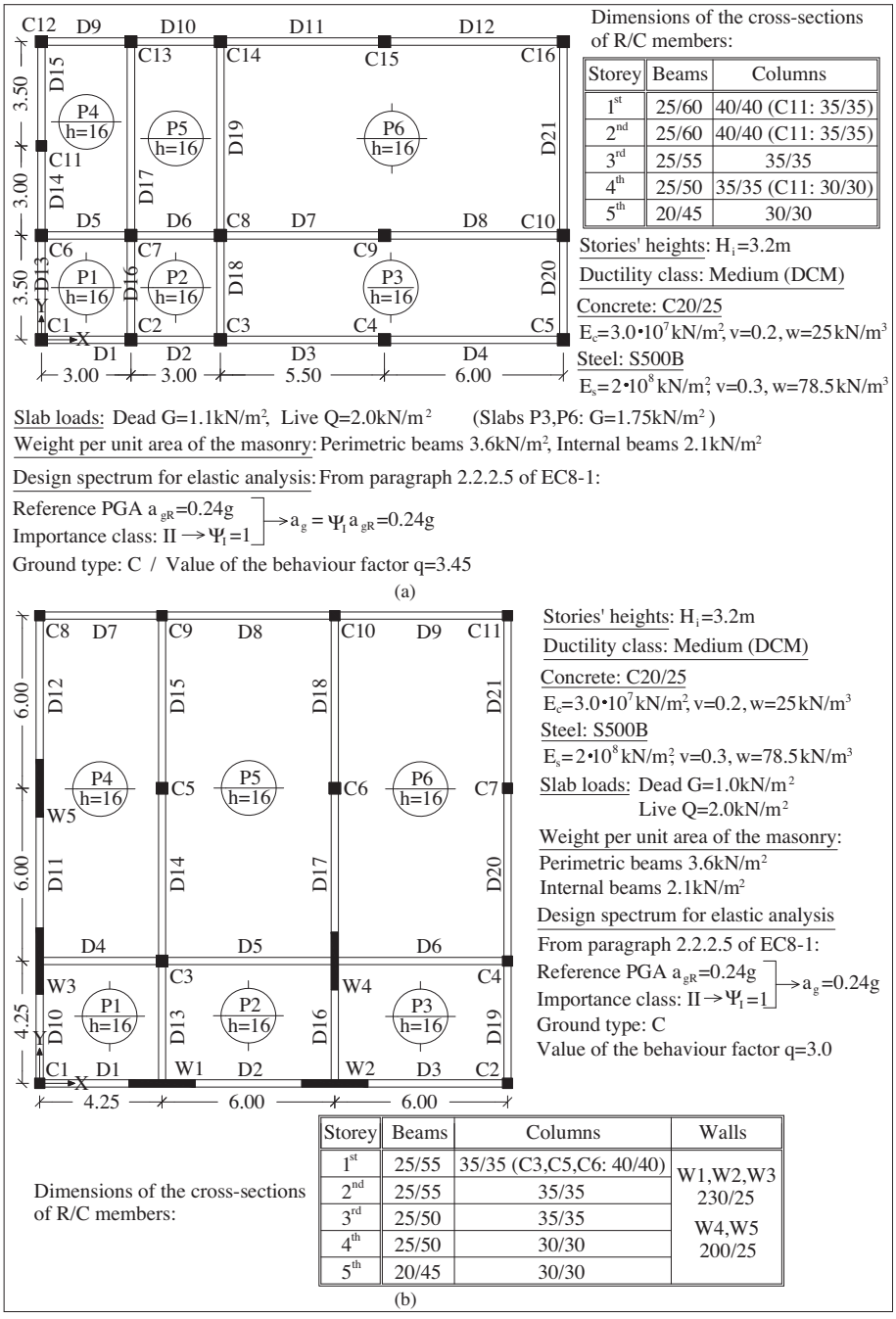

Fig. 2. 5-storey asymmetric buildings: (a) AFS and (b) AWS. Plan views, geometrical and design parameters.

common both in seismic codes and in literature for the definition of horizontal bidirectional ground motion characteristics [10,13–15,30] are used for each seismic excitation:

- Arithmetic Mean Value (AMV) : $IM_{AMV} = \frac{IM_1 + IM_2}{2}$ (2)
- Geometric Mean Value (GMV) : $IM_{GMV} = \sqrt{IM_1 \cdot IM_2}$ (3)
- Square Root of the Sum of the Squares (SRSS) : $IM_{SRSS} = \sqrt{IM_1^2 + IM_2^2}$ (4)
- Maximum Value : $IM_{MAX} = \max(IM_1, IM_2)$ (5)

where IM_1 and IM_2: values of the IMs determined for each one of the two horizontal components of the ground motion.

4. Description, design and modeling of the nonlinear behavior of the selected buildings

For the purposes of the present investigation, four 3D, R/C buildings, with data supplied in Figs. 1 and 2, are studied. All buildings are regular in elevation and have load resisting system that consists of elements arranged in two perpendicular directions (axes *X* and *Y*). The characteristics of the buildings investigated are:

- *Symmetric Frame System SFS (Fig. 1a):* Double-symmetric building without walls (frame system according to the structural

Table 2
First 8 natural periods and corresponding modal participating mass ratios of the 4 buildings investigated.

Mode	Period T (s)	X-axis (%)	Y-axis (%)	Period T (s)	X-axis (%)	Y-axis (%)
	SFS			*SWS*		
1	0.73	75.03	0.00	0.70	73.15	0.00
2	0.72	0.00	77.35	0.65	0.00	75.33
3	0.57	2.43	0.00	0.42	0.15	0.35
4	0.29	13.93	0.00	0.19	0.00	15.15
5	0.28	0.00	14.49	0.19	17.25	0.00
6	0.23	0.45	0.00	0.11	0.04	0.05
7	0.18	3.76	0.00	0.09	0.00	6.01
8	0.17	0.00	3.87	0.08	6.26	0.00
	AFS			*AWS*		
1	0.97	0.57	68.91	1.00	50.96	10.47
2	0.79	77.77	1.00	0.67	15.48	58.57
3	0.59	0.78	8.70	0.42	8.82	6.73
4	0.37	0.10	11.08	0.34	9.37	2.19
5	0.31	12.30	0.18	0.20	3.96	11.79
6	0.24	0.11	4.31	0.18	3.19	0.66
7	0.23	0.06	1.52	0.12	1.96	1.07
8	0.20	4.92	0.08	0.11	1.86	1.04

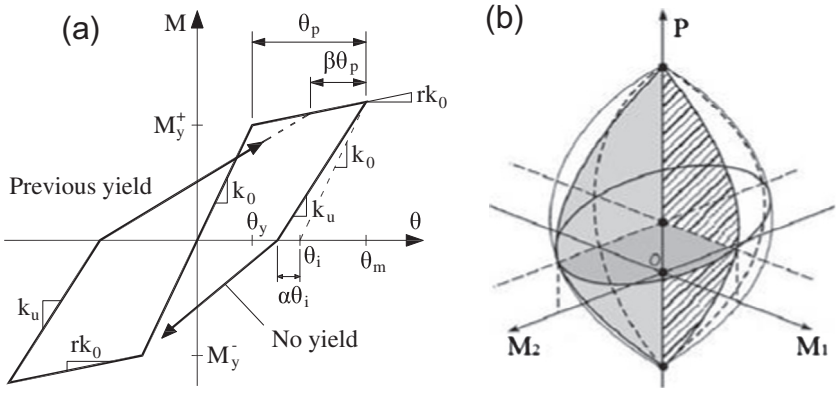

Fig. 3. Moment (M)–rotation (θ) relationship (a) and P–M_1–M_2 interaction diagram (b) [34].

types of the EC8 [11]). The building is regular in plan.

- *Symmetric Wall System SWS (Fig. 1b):* Double-symmetric building with walls that take approximately 65–70% of the base shear along both axes X and Y (wall system according to the structural types of the EC8 [11]). The building is regular in plan.
- *Asymmetric Frame System AFS (Fig. 2a):* Asymmetric building without walls (frame system according to the structural types of the EC8 [11]). The degree of the asymmetry is expressed in terms of the e_0/r ratio (where e_0 is the distance between the centre of stiffness and the centre of mass and r is the "torsional radius"). The value of this ratio along X-axis is $e_{0X}/r_X = 0.31 > 0.3$ and the respective ratio along Y-axis is equal to 0.06. So the building is irregular in plan [11].
- *Asymmetric Wall System AWS (Fig. 2b):* Asymmetric building with walls that take approximately 65–70% of the base shear along both axes X and Y (wall system according to the structural types of the EC8 [11]. The e_{0X}/r_X ratio along X-axis is equal to 0.4(>0.3) and the respective ratio along Y-axis is equal to 0.58(>0.3). So the building is irregular in plan [11].

All buildings were designed using the assumption that they behave as medium ductility class (DMC) buildings. Based on the above data, the process of determining the upper limit value of the behavior factor q of EC8 [11] led in the following values: Building SFS: maxq = 3.9, SWS: maxq = 3.0, AFS: maxq = 3.45 and AWS: maxq = 3.0.

The buildings were analyzed and designed on the basis of EC8 provisions [11]. As a result, the rigid diaphragm behavior of the floor slabs as well as the rigid zones in the joint regions of beams/columns and beams/walls were modeled. The wall behavior was modeled using an equivalent-column element placed at the wall cross section centroid. Moreover, the values of flexural and shear stiffness corresponding to cracked R/C elements were considered. Finally, the buildings were considered as fully fixed to the ground. The four structures were analyzed using the modal response spectrum analysis, as described in EC8 [11]. The R/C structural elements were designed following the clauses of EC2 [31] and EC8 [11]. It should be noted that the choice of the dimensions of the structural element cross-sections as well as of their reinforcement was made bearing in mind the optimum exploitation of the structural materials (steel and concrete). Therefore, the capacity ratios (CRs) of all critical cross-sections due to bending and shear are close to 1.0 (the mean value of CRs ranges between 0.92 and 0.96). For the design of the buildings the professional computer program RAF [32] was used. The first 8 natural periods as well as the corresponding modal participating mass ratios of all models are given in Table 2.

For the modeling of the buildings' nonlinear behavior, plastic hinges located at the column and beam ends as well as at the base of the walls were used. The material inelasticity of the structural members was modeled by means of the Modified Takeda hysteresis rule with zero post-yield stiffness r [33] (Fig. 3(a)).

It is important to notice that the effects of axial load–biaxial bending moment (P–M_1–M_2) interaction at column and wall hinges are taken into consideration by means of the P–M_1–M_2 interaction diagram shown in Fig. 3(b), which is implemented in the software used to conduct the analyses [34]. The yield moments as well as the parameters needed to determine the P–M_1–M_2 interaction diagram of the vertical elements' cross sections (Fig. 3(b)) are determined using appropriate software [35].

5. Damage indices – nonlinear time history analyses

The four buildings presented in the previous paragraph were analyzed by Nonlinear Time History Analysis (NTHA) for each one of the 64 earthquake ground motions taking into account the design vertical loads of the structures. The analyses were performed with the aid of the computer program Ruaumoko [34]. Furthermore, as the seismic incident angle with regard to structural axes is unknown, the two horizontal uncorrelated accelerograms of each ground motion were applied along horizontal orthogonal axes forming with the structural axes an angle $\theta = 0°, 5°, 10°, \ldots, 355°$. Thus, for each building and each pair of accelerograms 72 orientations were considered. As a consequence a total of 18,432 NTHA (4 buildings × 64 earthquake records × 72 incident angles) were conducted in the present study.

For each ground motion and incident angle, the damage state of the four buildings was determined. The seismic performance is expressed in the form of the following parameters: (i) the Maximum Interstorey Drift Ratio (MIDR), (ii) the Average Interstorey Drift Ratio (AIDR) and (iii) the Overall Structural Damage Index (OSDI). The value of each one of the above parameters for incident angle 0° (common practice of applying the accelerograms along the structural axes) as well as their maximum value over the 72 incident angles was determined.

The aforementioned structural response parameters were chosen, since they lump the existing damage in all the cross-sections in a single value, which can be easily correlated to scalar seismic intensity measures. So, they have been used by many researchers for the assessment of the inelastic response of structures [2–4,6–9,36].

The MIDR, which is generally considered an effective indicator of global structural and nonstructural damage of R/C buildings, e.g. [37,38] corresponds to the maximum drift among the four perimeter frames. In order to determine the AIDR, the horizontal roof displacement of each perimeter frame was computed and divided by the total height of the building. Then, the maximum value among the four perimeter frames was considered.

Moreover, the overall structural damage index (OSDI) of the buildings was determined. Note that, in general, damage indices estimate quantitatively the degree of seismic damage that a cross-section as well as a whole structure has suffered. In the present study, the OSDI was computed as a weighted average of the local damage indices at the ends of each structural element. The dissipated energy was used as a weight factor (Eq. (6)) [2,3,36,39]:

$$\mathrm{OSDI} = \sum_{i=1}^{n}\left[\mathrm{LDI}_i \cdot \left(E_{Ti} \Big/ \sum_{i=1}^{n} E_{Ti}\right)\right] \tag{6}$$

where LDI_i is the local damage index at cross section i (Eq. (7)), E_{Ti} is the energy dissipated at the cross section i and n is the number of cross sections at which the local damage is computed. For the LDI, the widely used Park and Ang damage index [40] modified by Kunnath et al. [41] has been used. The advantages of this damage index are its simplicity and the fact that it has been calibrated against a significant amount of observed seismic damage. It is also important to mention that the Park and Ang damage index was tested experimentally. At a given cross section the local damage index (LDI) is given by Eq. (7):

$$\mathrm{LDI} = \frac{\varphi_m - \varphi_y}{\varphi_u - \varphi_y} + \left(\frac{\beta}{M_y \cdot \varphi_u}\right) \cdot E_T \tag{7}$$

where φ_m is the maximum curvature observed during the load history, φ_u is the ultimate curvature capacity, φ_y is the yield curvature, E_T is the dissipated hysteretic energy, M_y is the yield moment of the cross section and β is a dimensionless constant determining the contribution of cyclic loading to damage, which is taken equal to 0.5 for the analyses conducted.

6. Comparative assessment of the results

6.1. Computation of correlation coefficients

Correlation coefficients are determined to express the grade of interdependency between the examined ground motion IMs and the damage measures of the four buildings. As a first step, the Kolmogorov–Smirnov test was used in order to identify whether the input parameters follow a normal distribution. For the selected set of ground motions, this test showed that, with a 5% error, the examined quantities do not follow the normal distribution. So,

Table 3
Correlation among ground motion intensity measures determined using the arithmetic mean value of the two horizontal seismic component.

Intensity measures	PGA	PGV	PGD	PGV/PGA	SMA	SMV	EDA	a_{rms}	v_{rms}	d_{rms}	I_a	I_c	SED	CAV	ASI	VSI	HI	EPA
PGA	1.000																	
PGV	0.521	1.000																
PGD	0.156	0.802	1.000															
PGV/PGA	−0.338	0.549	0.721	1.000														
SMA	0.853	0.577	0.340	−0.146	1.000													
SMV	0.364	0.817	0.847	0.540	0.550	1.000												
EDA	0.999	0.518	0.152	−0.340	0.846	0.356	1.000											
a_{rms}	0.830	0.604	0.318	−0.104	0.873	0.549	0.825	1.000										
v_{rms}	0.355	0.862	0.874	0.604	0.501	0.902	0.347	0.609	1.000									
d_{rms}	0.061	0.703	0.952	0.701	0.268	0.811	0.056	0.252	0.842	1.000								
I_a	0.766	0.761	0.535	0.107	0.874	0.719	0.761	0.882	0.701	0.444	1.000							
I_c	0.806	0.727	0.468	0.039	0.899	0.679	0.799	0.947	0.689	0.388	0.983	1.000						
SED	0.272	0.865	0.940	0.686	0.441	0.907	0.267	0.458	0.926	0.868	0.684	0.620	1.000					
CAV	0.417	0.735	0.700	0.409	0.598	0.783	0.414	0.550	0.715	0.627	0.839	0.756	0.838	1.000				
ASI	0.930	0.510	0.148	−0.303	0.872	0.426	0.929	0.894	0.381	0.056	0.832	0.877	0.303	0.490	1.000			
VSI	0.538	0.931	0.767	0.502	0.598	0.803	0.537	0.642	0.864	0.666	0.768	0.741	0.848	0.703	0.534	1.000		
HI	0.450	0.909	0.822	0.575	0.540	0.832	0.448	0.582	0.892	0.728	0.723	0.689	0.895	0.710	0.451	0.981	1.000	
EPA	0.932	0.519	0.157	−0.295	0.873	0.432	0.932	0.897	0.388	0.065	0.837	0.881	0.312	0.497	0.999	0.543	0.459	1.000

for the evaluation of the correlation between the investigated parameters, the Spearman rank correlation coefficient was adopted.

The Spearman's rank correlation coefficient is used as an index to assess how well the relationship between two variables X and Y can be described using a monotonic function. Its value ranges from -1 to 1. The values 1 and -1 indicate that each of the variables is a perfect monotone function of the other while 0 indicates no association between the ranks of the two variables. The Spearman rank correlation coefficient between two variables X and Y is given by Eq. (8):

$$\rho_{\text{Spearman}} = 1 - \frac{6\sum_{i=1}^{N} D^2}{N\left(N^2 - 1\right)} \tag{8}$$

where D: differences between the ranks of corresponding values of X_i and Y_i and N: number of pairs of values (X, Y) in the data.

6.2. Correlation among earthquake intensity measures

Table 3 presents the Spearman rank correlation coefficients for the examined ground motion IMs. As it was mentioned in Section 3, four different expressions were used (Eqs. (2)–(5)) to combine the two IMs corresponding to each one of the two horizontal orthogonal seismic components into a single parameter. The numerical assessment of the IMs revealed that the values of the correlation coefficients determined using these expressions are very similar. Table 3 shows the results produced with the aid of the AMV of the two horizontal components of the strong motion (Eq. (2)). The results produced with the aid of GMV, SRSS and Maximum Value are not presented for brevity. Furthermore, it must be noticed that the correlation coefficients for $S_a(T_1)$ are not presented in the table, since they depend on the building analyzed.

We can see (Table 3) that PGV, I_a, I_c, VSI and HI show the strongest correlation with the majority of the IMs. On the contrary, the IMs that show the smallest correlation coefficients are PGV/PGA and d_{rms}. From the same table it is also evident the high correlation between acceleration related measures, while their correlation with velocity and displacement related measures is weak. On the other hand, velocity related measures correlate well between each other as well as with displacement related measures. Finally, displacement related measures are strongly correlated between each other.

6.3. Correlation among damage measures

In order to investigate the correlation between the three different measures of the buildings' damage state adopted in the present study, the Spearman's correlation coefficients were determined. In Table 4 the correlation coefficients computed for the maximum values of the damage measures over the 72 seismic incident angles are given. In Table 5 the correlation coefficients corresponding to accelerograms applied along the structural axes (incident angle equals to 0°) are given.

Table 4
Correlation among structural damage measures (maximum values over the 72 incident angles).

	Damage measures	OSDI	MIDR	AIDR
SFS	OSDI	1.000		
	MIDR	0.810	1.000	
	AIDR	0.715	0.960	1.000
SWS	OSDI	1.000		
	MIDR	0.776	1.000	
	AIDR	0.654	0.904	1.000
AFS	OSDI	1.000		
	MIDR	0.686	1.000	
	AIDR	0.638	0.931	1.000
AWS	OSDI	1.000		
	MIDR	0.055	1.000	
	AIDR	−0.021	0.930	1.000

Table 5
Correlation among structural damage measures (values for incident angle 0°).

	Damage measures	OSDI	MIDR	AIDR
SFS	OSDI	1.000		
	MIDR	0.887	1.000	
	AIDR	0.935	0.924	1.000
SWS	OSDI	1.000		
	MIDR	0.870	1.000	
	AIDR	0.856	0.965	1.000
AFS	OSDI	1.000		
	MIDR	0.853	1.000	
	AIDR	0.798	0.915	1.000
AWS	OSDI	1.000		
	MIDR	0.725	1.000	
	AIDR	0.704	0.975	1.000

Table 4 clearly indicates that MIDR and AIDR show very strong correlation between each other and small-to-moderate correlation with OSDI. This result can be attributed to the fact that both MIDR and AIDR are determined considering displacement demands, while the determination of OSDI is based on the deformation demands of the structural elements. Furthermore, notice that OSDI exhibits higher correlation with MIDR than AIDR for all the investigated buildings. Finally, we can see that the values of correlation coefficients between OSDI and the other two damage indices are larger for the symmetric buildings, whereas there is no correlation at all in case of the asymmetric frame-wall system.

From Table 5 we can see that ignoring the incident angle of the seismic input does not alter significantly the values of correlation coefficients between MIDR and AIDR. On the other hand, with regard to correlation between OSDI and the two damage indicators based on displacement demands, it is evident that this correlation is stronger in case of applying the accelerograms along the structural axes. The above deduction is particularly obvious for the AWS building.

6.4. Correlation between earthquake intensity measures and structural response

The relative adequacy of the examined seismic IMs as indicators of the structural response is evaluated by the Spearman's rank correlation coefficient. More specifically, the maximum value of each one of the damage measures over the 72 incident angles produced by the ground motions given in Table 1 was correlated with the 19 IMs presented in Section 3. Figs. 4–7 present the Spearman's rank correlation coefficients between the damage indices and the seismic IMs for the four buildings. The figures illustrate the results produced by the four different expressions used to combine in a single parameter the two separate values of IMs corresponding to the two horizontal seismic components (Eqs. (2)–(5)).

From these figures it can be concluded that, for the vast majority of the IMs the correlation with the structural damage state is stronger when the damage measures based on displacements demands (MIDR and AIDR) are used as response parameters. This conclusion is more obvious for the frame-wall systems, SWS and AWS (Figs. 5 and 7). A comparison between MIDR and AIDR does not reveal a general trend, since the interdependency between them and the IMs depends on both the seismic intensity measure as well as on the building characteristics. See for example that EDA and a_{rms} correlate better with MIDR than AIDR for the two

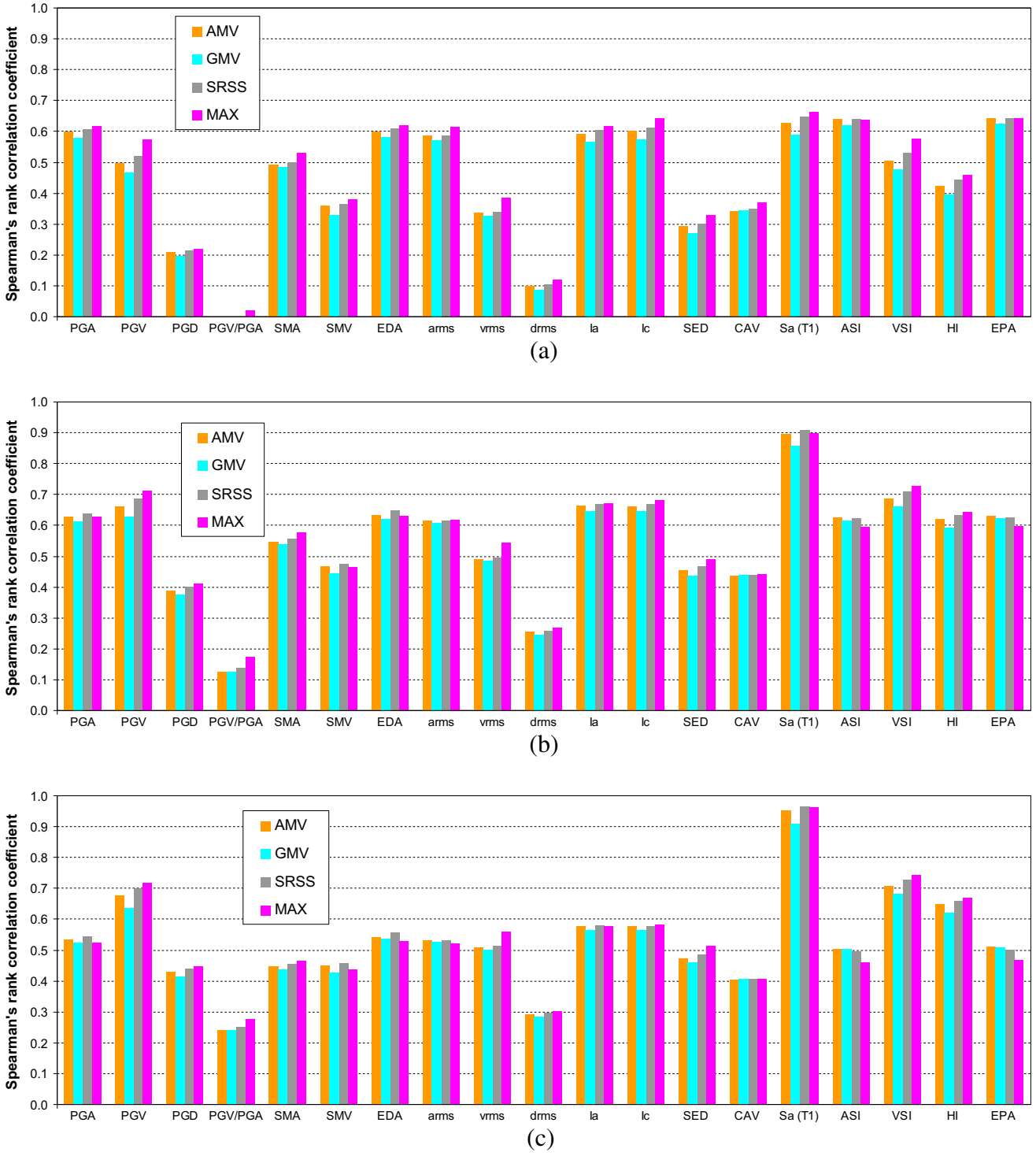

Fig. 4. Spearman's rank correlation coefficients between seismic intensity measures and maximum damage indices over all incident angles (OSDI (a), MIDR (b), AIDR (c)) for SFS.

frame buildings (Figs. 4 and 6). On the contrary, EDA and a_{rms} correlate better with AIDR than MIDR for the SWS (Fig. 5), whereas, in case of the AWS the two IMs (EDA and a_{rms}) have almost the same grade of correlation (Fig. 7). However, we can see that some IMs, such as PGV/PGA and $S_a(T_1)$, exhibit higher correlation with AIDR than MIDR for all the investigated buildings.

The comparative assessment of the seismic intensity measures evaluated in the present study shows that $S_a(T_1)$ has the strongest correlation with MIDR and AIDR, followed by VSI, PGV and HI (Figs. 4b, c, 5b, c, 6b, c and 7b, c). The only exception is the correlation coefficient between HI and MIDR for the SFS (Fig. 4b), which has smaller value than the values produced by other IMs such as I_a and I_c. Moreover, the correlation between MIDR or AIDR and the 19 IMs examined herein is of the same order for SFS, AFS and AWS and slightly smaller for SWS.

Figs. 8–11 illustrate the relationship between the spectral acceleration at the fundamental period and the two damage measures which are based on deformation demands (i.e. MIDR and AIDR).

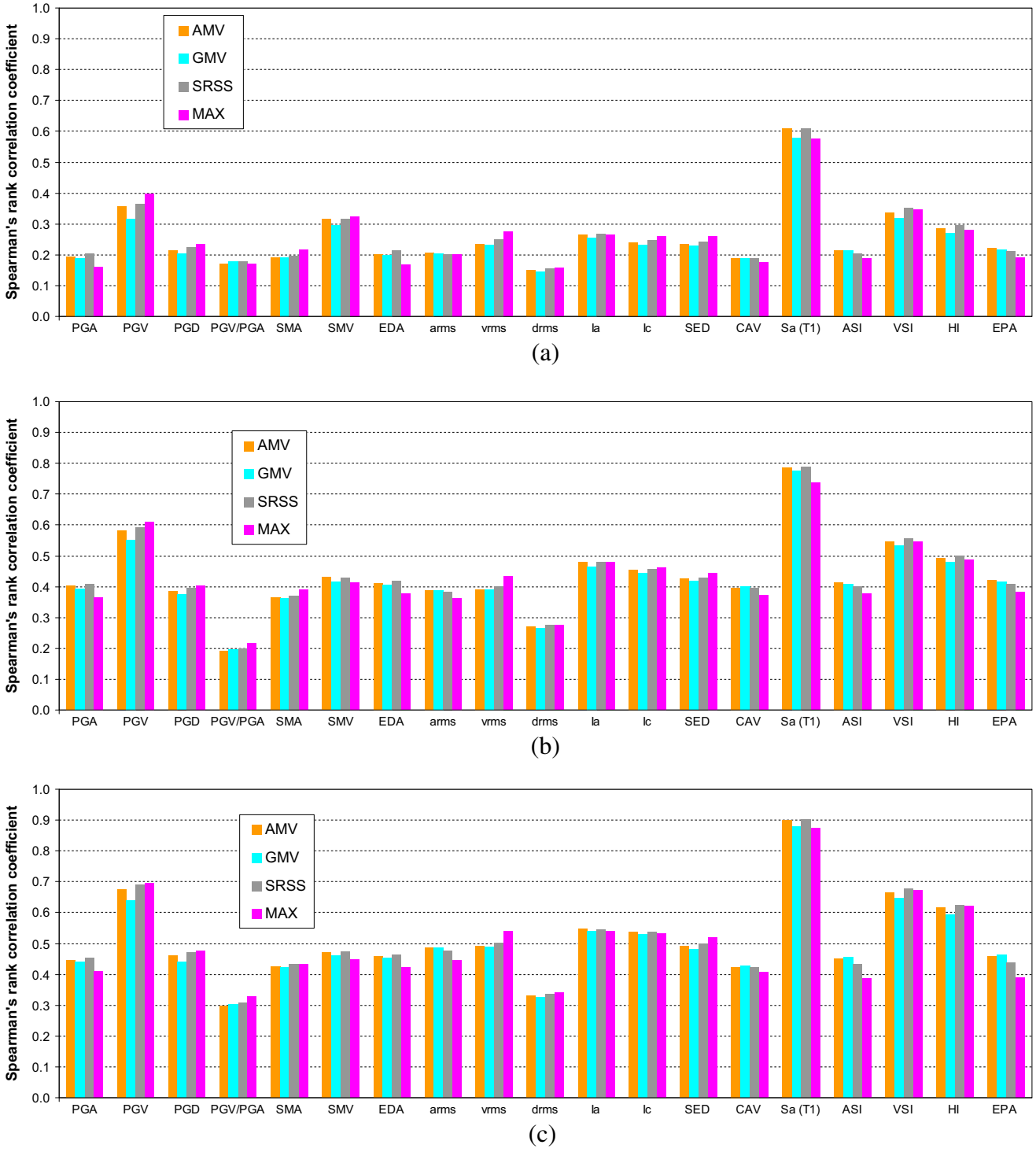

Fig. 5. Spearman's rank correlation coefficients between seismic intensity measures and maximum damage indices over all incident angles (OSDI (a), MIDR (b), AIDR (c)) for SWS.

Note that the correlation between $S_a(T_1)$ and MIDR or AIDR can be very high even for the asymmetric in plan buildings (Spearman's correlation coefficient can reach the value of 0.96 in case of AIDR of AFS, Fig. 6c). The effectiveness of $S_a(T_1)$ as indicator of the seismic motion destructiveness is in agreement with previous studies [1,2,15]. This is due to the fact that it is the only one of the investigated earthquake intensity measures that incorporates structural information. Furthermore, as it has been observed by Riddell [5], velocity related indices, such as PGV, VSI and HI, are more effective for the medium-to-long period structures ($T_1 > 0.5$ s). This observation is also true for the herein investigated buildings, which have fundamental period longer than 0.5 s (see Table 2).

The results shown in Figs. 4–7 also indicate that the interdependency between IMs and OSDI is strongly influenced by the load resisting system. In particular, the values of Spearman's rank correlation coefficients are larger for the frame systems than the frame-wall systems.

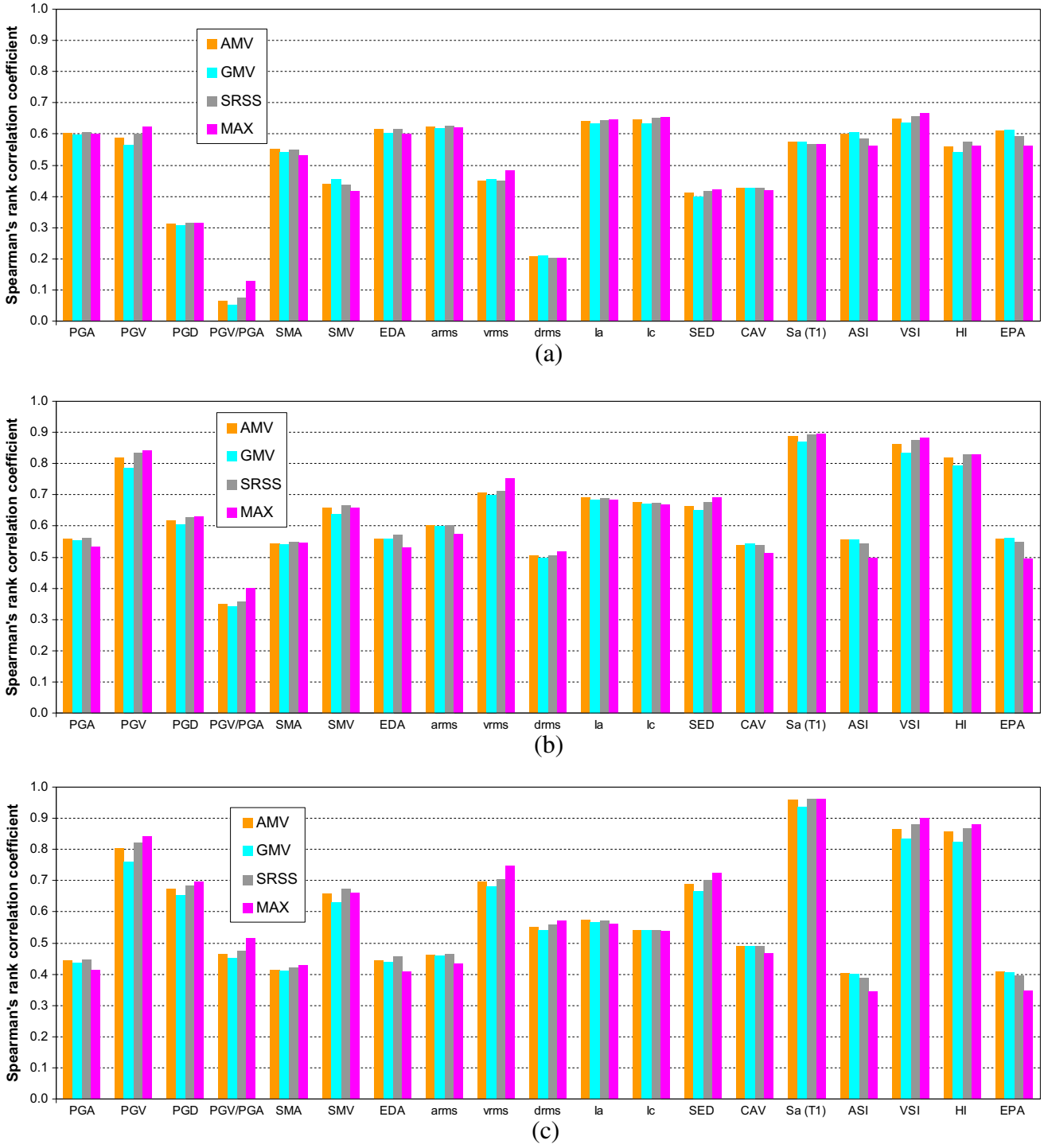

Fig. 6. Spearman's rank correlation coefficients between seismic intensity measures and maximum damage indices over all incident angles (OSDI (a), MIDR (b), AIDR (c)) for AFS.

Furthermore, Figs. 4a and 6a depict that, for the selected frame systems, there are several IMs, which exhibit medium correlation with OSDI, since the respective correlation coefficients can reach the value of 0.6. Such seismic IMs are PGA, EDA, a_{rms}, I_a, I_c, ASI and EPA. Nonetheless, no IM seems to be the best indicator of structural performance because all of them have similar rank correlation with OSDI.

As far as the frame-wall systems are concerned, from Figs. 5a and 7a it is evident that OSDI shows poor correlation with the majority of IMs for the SWS and does not correlate at all with them in case of AWS. However, as an exception, OSDI correlates moderately (the Spearman's rank correlation coefficient is 0.61) with $S_a(T_1)$ in case of the SWS (Fig. 5a). The relationships between $S_a(T_1)$ and OSDI for the frame-wall systems investigated (SWS and AWS) are shown in Figs. 12 and 13.

The inadequacy of the seismic IMs to describe the expected OSDI of the selected frame-wall systems is attributed to the assumptions and the inherent uncertainties of the definition of

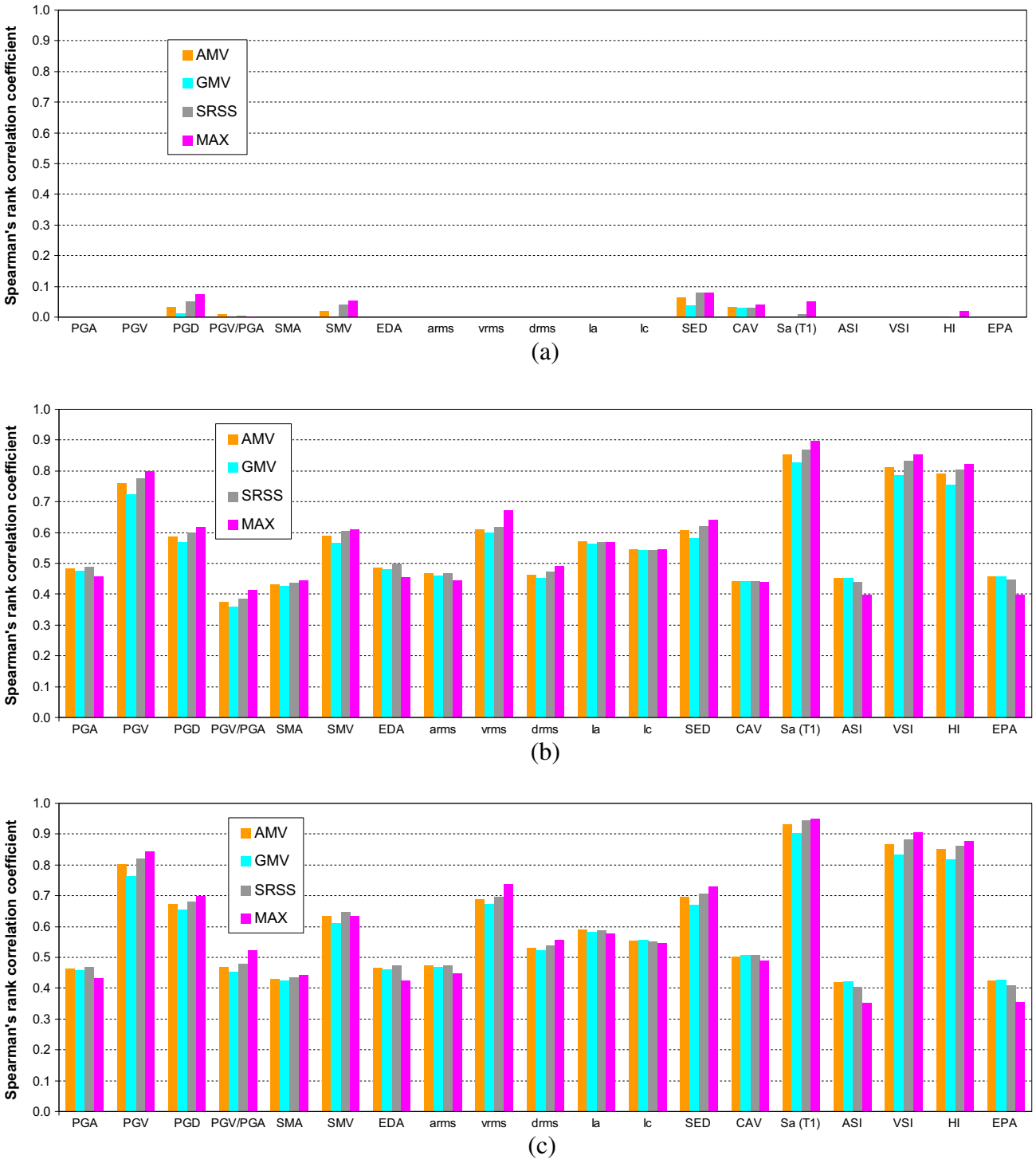

Fig. 7. Spearman's rank correlation coefficients between seismic intensity measures and maximum damage indices over all incident angles (OSDI (a), MIDR (b), AIDR (c)) for AWS.

the OSDI (Eq. (6)), as well as to the damage distribution exhibited by these buildings. In particular, the analyses showed that, for a large number of earthquakes, the damage observed in the frame-wall systems studied herein was restricted to a single column or wall, although the rest of structural elements remained elastic. In this case, the value of the OSDI is very large, since it takes into account only the damaged cross sections (Eq. (6)) and ignores the elastic frame elements, where the dissipated energy is zero. Such a result is misleading, because in this case large OSDI indicates very significant structural damage of the whole building, ignoring the fact that the damage was restricted to a single structural element.

Figs. 4–7 show that in most cases the least effective IMs are the PGV/PGA and the d_{rms}. Of particular interest is also the fact that the influence of the variant definitions of a single intensity parameter corresponding to the two horizontal seismic components on the

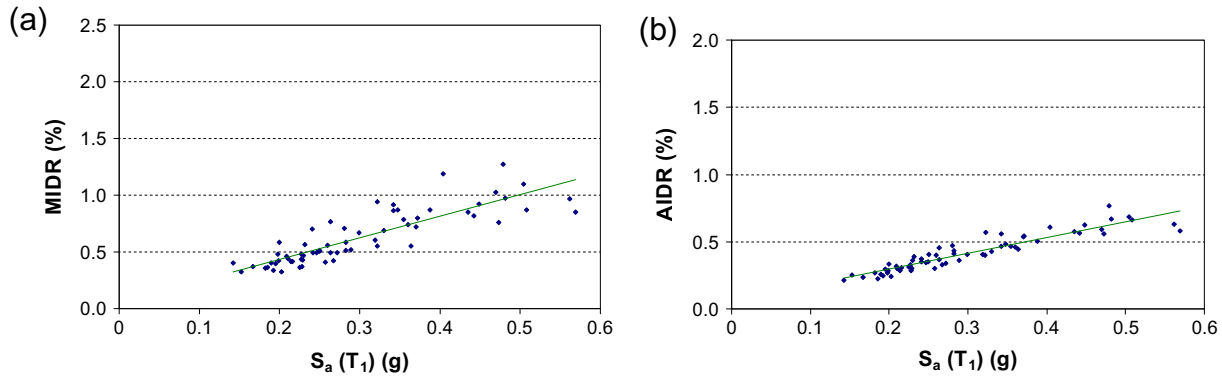

Fig. 8. Relationship between $S_a(T_1)$ and MIDR (a) or AIDR (b) for the SFS when the AMV of the horizontal seismic components is used.

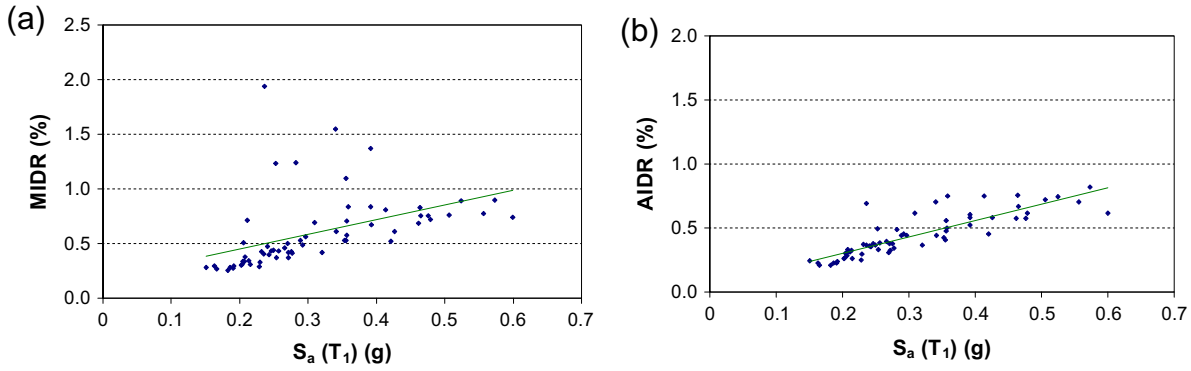

Fig. 9. Relationship between $S_a(T_1)$ and MIDR (a) or AIDR (b) for the SWS when the AMV of the horizontal seismic components is used.

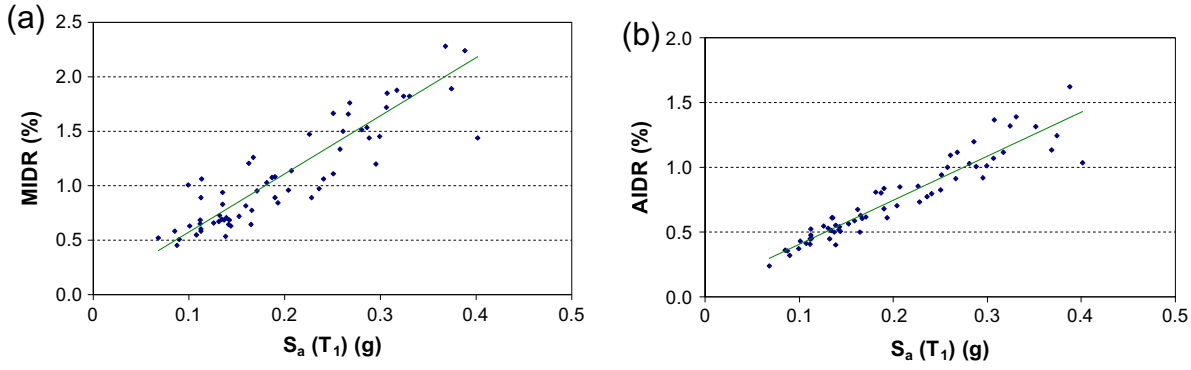

Fig. 10. Relationship between $S_a(T_1)$ and MIDR (a) or AIDR (b) for the AFS when the AMV of the horizontal seismic components is used.

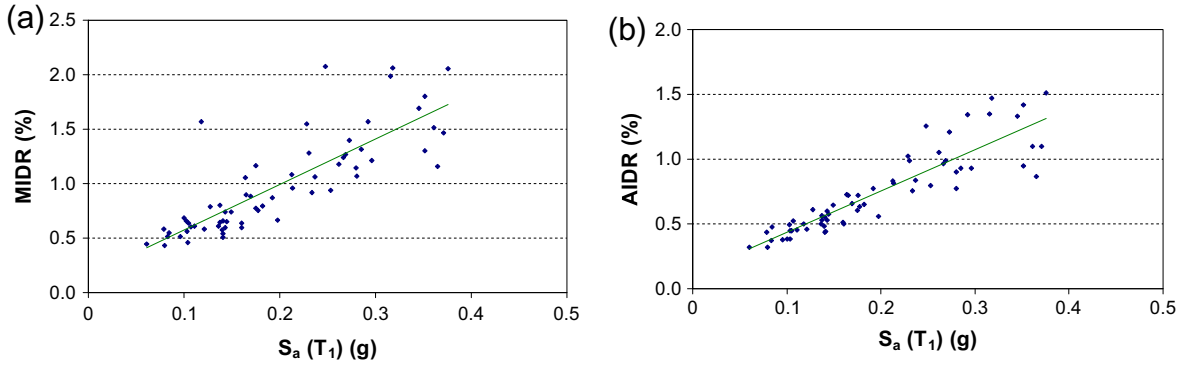

Fig. 11. Relationship between $S_a(T_1)$ and MIDR (a) or AIDR (b) for the AWS when the AMV of the horizontal seismic components is used.

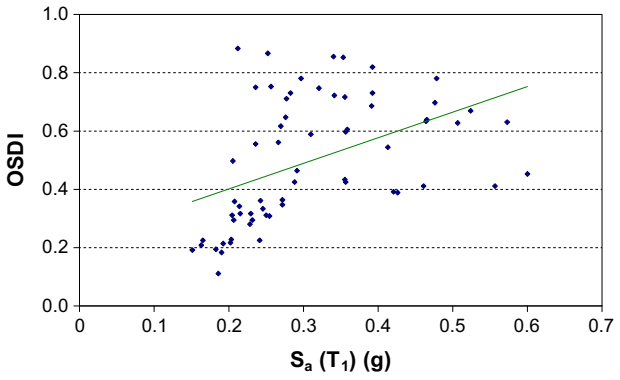

Fig. 12. Relationship between $S_a(T_1)$ and OSDI for the SWS when the AMV of the horizontal seismic components is used.

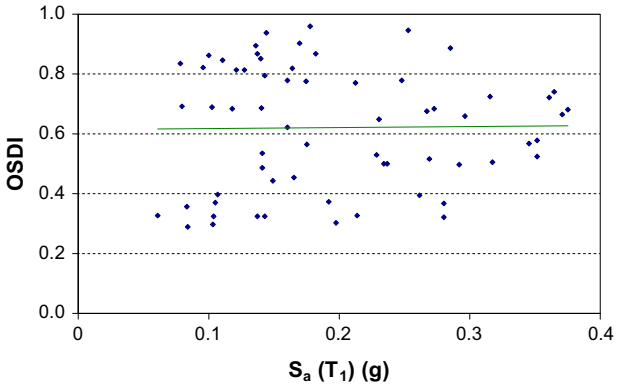

Fig. 13. Relationship between $S_a(T_1)$ and OSDI for the AWS when the AMV of the horizontal seismic components is used.

correlation coefficients between IMs and damage measures is almost negligible. The above conclusion also applies for all the IMs, damage measures and buildings considered in the present study.

Furthermore, the Spearman's correlation coefficients between the IMs and the values of the three damage response parameters for seismic incident angle equal to 0° degrees (that is the common case in engineering practice) were also computed. Indicatively, the results for the building AWS are presented in Fig. 14.

We can see that the Spearman's rank correlation coefficients between IMs and OSDI are much larger for seismic input along the structural axes than the ones determined when variable orientations of the seismic motion were taken into consideration. This is more evident for the asymmetric buildings and particularly for AWS (Figs. 7a and 14a) for which the correlation coefficients between IMs and OSDI are negligible (Fig. 7a). Note that for some IMs the correlation between them and OSDI is stronger than the one produced for response parameters based on displacements demands (MIDR and AIDR). See for example I_a and CAV of the building AWS (Fig. 14). Also we see (Fig. 14) that the correlation coefficients have slightly larger values than the ones produced for the critical seismic incident angle (that is the one causing the most severe damage over all incident angles (Fig. 7)). The general observations based on the results of Figs. 4–13 are also valid when the seismic motion is applied along the structural axes. More specifically, when MIDR or AIDR is used as a damage measure, the first-mode spectral acceleration and the velocity related IMs (VSI, PGV and HI) exhibit the strongest correlation with the structural response. However, this is not always the case when OSDI is adopted as a descriptor of the seismic performance. We can see that there are some other IMs that also exhibit strong correlation with OSDI (e.g. SED and v_{rms}, Fig. 14).

7. Conclusions

In this paper the correlation between 19 ground motion IMs and the damage state of four medium-rise 3D R/C buildings is investigated. The structural performance was evaluated by NTHA using 64 bidirectional ground motions and taking into consideration the orientation of the seismic input with regard to structural axes. The structural damage state was expressed in terms of the overall structural damage index (OSDI), the maximum interstorey drift ratio (MIDR) and the average interstorey drift ratio (AIDR). The comparative assessment of the results has led to the following conclusions:

- Concerning the interdependency of the examined IMs between each other, the analyses revealed that PGV, I_a, I_c, VSI and HI show the highest correlation with the majority of the IMs. Moreover, acceleration related measures exhibit strong correlation between each other, while their interdependency with velocity and displacement related measures is weak. On the other hand, velocity related measures correlate well between each other as well as with displacement related measures.
- With regard to the correlation between the seismic damage measures in the case of accounting for the variable earthquake orientation, it was shown that MIDR and AIDR exhibit very strong correlation between each other and small-to-moderate correlation with OSDI. Moreover, the correlation between OSDI and the other two damage indices is higher for the symmetric buildings compared to the asymmetric ones. When the accelerograms are applied along the structural axes the interdependency between OSDI and MIDR or AIDR is much stronger.
- When the incident angle is taken into consideration the correlation between the examined IMs and MIDR or AIDR is higher than the correlation between them and OSDI. This conclusion is more obvious for the frame-wall systems. However, when the horizontal components of the ground motion are applied along the structural axes, there are cases where the correlation between certain IMs and OSDI is stronger than the one produced when the response parameters based on displacements demands (MIDR and AIDR) are used.
- When the MIDR or AIDR is used as response indicator, the correlation coefficients are larger for the $S_a(T_1)$, followed by VSI, PGV and HI. On the other hand, the least effective seismic IMs are, in most cases, the ratio PGV/PGA and d_{rms}. However, this is not always the case when OSDI is adopted as a descriptor of the seismic performance.
- When different incident angles are taken into account the majority of IMs show medium correlation with OSDI in case of the frame systems, whereas no certain seismic intensity measure seems to be the most efficient. Regarding the frame-wall systems investigated, the analyses revealed that the correlation between OSDI and the examined ground motion IMs is weak for the SWS and negligible for the AWS.
- The Spearman's rank correlation coefficients between OSDI and the majority of IMs are larger for the case of applying the accelerograms along the structural axes than the ones determined when variable orientations of the seismic motion were taken into consideration.

It must be noted that the aforementioned conclusions are valid for the buildings and ground motions used in the present study.

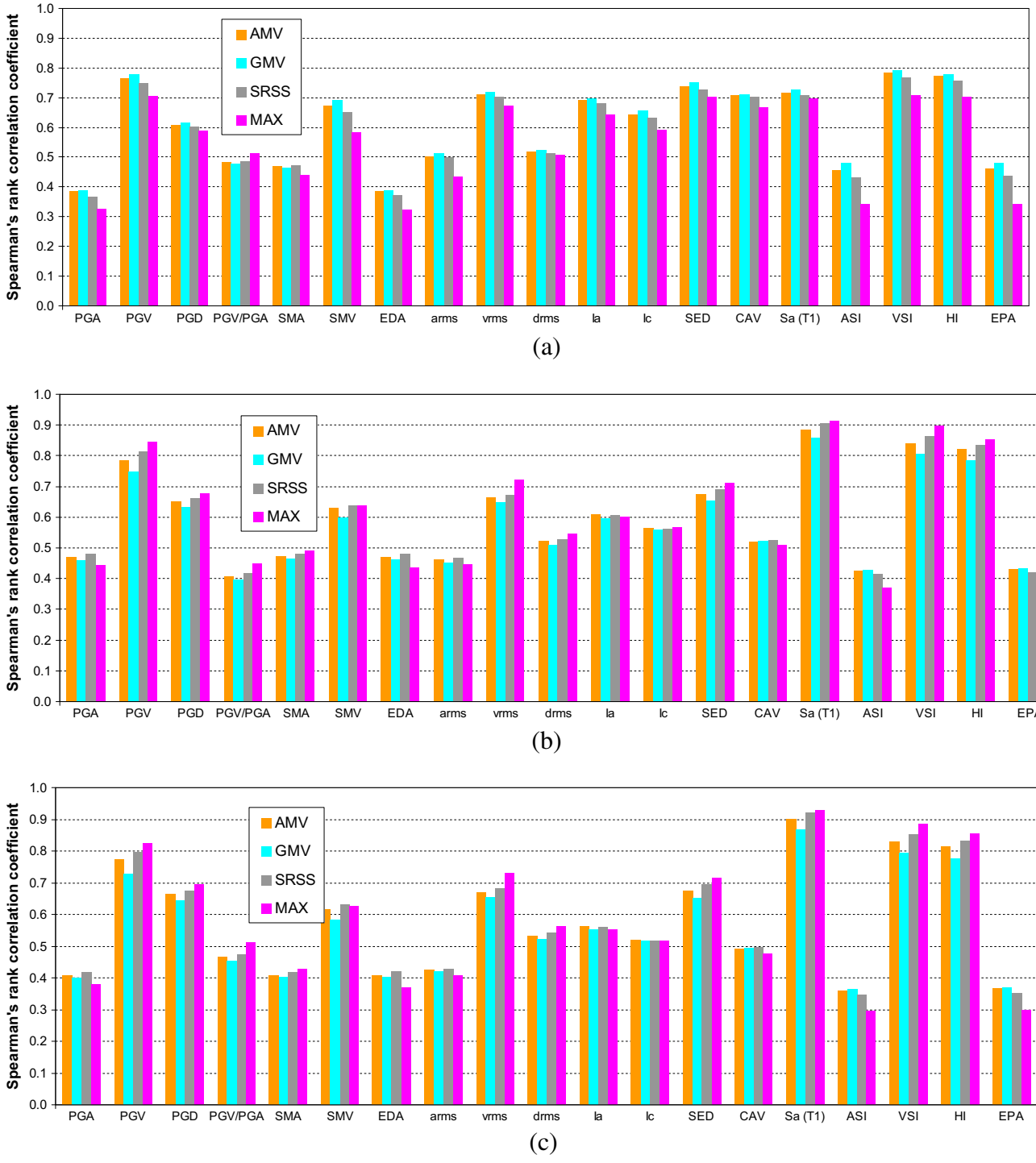

Fig. 14. Spearman's rank correlation coefficients between seismic intensity measures and maximum damage indices for incident angle 0° (OSDI (a), MIDR (b), AIDR (c)) for AWS.

However, they provide a good insight into the correlation between damage state to 3D, R/C buildings under bidirectional excitation and the known IMs. Moreover, they provide significant information relative to the efficiency of the commonly used damage indicators as well as the influence of the seismic orientation with regard to structural axes. In order to expand them to other structural systems, further investigation is necessary. In particular, the research can be extended to low- and high-rise buildings with various degrees of asymmetry (e_0/r ratio), as well as to structures with different ratio of the *base shear* carried by the walls. Moreover, earthquake records with different characteristics (e.g. magnitude, epicentral distance, frequency content) could be considered or, alternatively, the ground motions can be grouped to ensembles of records based on their duration or frequency content.

Acknowledgement

This study was financially supported by A.U.Th. Research Committee (Fellowships of Excellence for Postgraduate Studies 2013).

References

[1] Elenas A. Interdependency between seismic acceleration parameters and the behaviour of structures. Soil Dyn Earthq Eng 1997;16:317–22.
[2] Elenas A. Correlation between seismic acceleration parameters and overall structural damage indices of buildings. Soil Dyn Earthq Eng 2000;20:93–100.
[3] Elenas A, Meskouris K. Correlation study between seismic acceleration parameters and damage indices of structure. Eng Struct 2001;23:698–704.
[4] Liao W-I, Hsiung C, Wan S. Earthquake responses of RC moment frames subjected to near-fault ground motions. Struct Des Tall Build 2001;10:219–29.
[5] Riddell R. On ground motion intensity indices. Earthq Spect 2007;23:147–73.
[6] San A, Hzurbaba K, Yildirim Y. A correlation study between ground motion parameters and damage during Kocaeli Earthquake. In: Proceedings of 16th ASCE engineering mechanics conference, Seattle; 2003.
[7] Yakut A, Yilmaz H. Correlation of deformation demands with ground motion intensity. J Struct Eng 2008;134(12):1818–28.
[8] Masi A, Vona M, Mucciarelli M. Selection of natural and synthetic accelerograms for seismic vulnerability studies on reinforced concrete frames. J Struct Eng 2011;137:367–78.
[9] Ye Lieping, Ma Qianli, Miao Zhiwei, Guan Hong, Zhuge Yan. Numerical and comparative study of earthquake intensity indices in seismic analysis. Struct Des Tall Spect Build 2013;22:362–81.
[10] ASCE/SEI 41-06. Seismic rehabilitation of existing buildings. Reston (VA): American Society of Civil Engineers; 2008.
[11] Eurocode 8 (1998-1). Design provisions for earthquake resistance of structures. European Committee for Standardization; 2003.
[12] UBC Vol. 2. Structural engineering design provisions. Whittier (CA): International Conference of Building Officials (ICBO); 1997.
[13] FEMA 356. Prestandard and commentary for the seismic rehabilitation of buildings. Washington (DC): Federal Emergency Management Agency; 2000.
[14] NEHRP. Recommended provisions for seismic regulations for new buildings and other structures, FEMA450. Washington (DC): Building Seismic Safety Council; 2003.
[15] Cantagallo C, Camata G, Spacone E, Corotis R. The variability of deformation demand with ground motion intensity. Probabilist Eng Mech 2012;28:59–65.
[16] Lucchini A, Mollaioli F, Monti G. Intensity measures for response prediction of a torsional building subjected to bi-directional earthquake ground motion. Bull Earthq Eng 2011;9:1499–518.
[17] Athanatopoulou A. Critical orientation of three correlated seismic components. Eng Struct 2005;27(1):301–12.
[18] Kostinakis K, Athanatopoulou A, Avramidis I. Influence of orientation of recorded ground motion components on the reinforcing steel area in concrete frame elements. In: Proceedings of 9th US national and 10th Canadian conference on earthquake engineering, 25–29 July, Toronto, Canada, 2010, Paper No: 1066.
[19] Kostinakis K, Athanatopoulou A, Avramidis I. Orientation effects of horizontal seismic components on longitudinal reinforcement in R/C Frame elements. Nat Hazard Earthq Syst Sci 2012;12:1–10.
[20] Fontara I-K, Kostinakis K, Athanatopoulou A. Some issues related to the inelastic response of buildings under bi-directional excitation. In: Proceedings of 15th world conference on earthquake engineering, Paper No: 3715, Lisbon, Portugal, September 24–28, 2012.
[21] Kostinakis K, Athanatopoulou A, Avramidis I. Evaluation of inelastic response of 3D single-story R/C frames under bi-directional excitation using different orientation schemes. Bull Earthq Eng 2013;11:637–61.
[22] Lagaros ND. The impact of the earthquake incident angle on the seismic loss estimation. Eng Struct 2010;32:1577–89.
[23] Lucchini A, Monti G, Kunnath S. Nonlinear response of two-way asymmetric single-story building under biaxial excitation. J Struct Eng 2011;137(1):34–40.
[24] Rigato A, Medina R. Influence of angle of incidence on seismic demands for inelastic single-storey structures subjected to bi-directional ground motions. Eng Struct 2007;29:2593–601.
[25] Fontara I-K, Athanatopoulou A, Avramidis I. Correlation between ground motion intensity measures and damage indices in case of an asymmetric 3D R/C building. In: Proceedings of 7th GRACM international congress on computational mechanics, Athens, Greece; 2011.
[26] Pacific Earthquake Engineering Research Centre (PEER). Strong motion database <http://peer.berkeley.edu/smcat/>; 2003.
[27] European Strong-Motion Database. <http://www.isesd.hi.is/ESD Local/frameset.htm. 2003>.
[28] Penzien J, Watabe M. Characteristics of 3-D earthquake ground motions. Earthq Eng Struct Dyn 1975;3:365–73.
[29] Kramer SL. Geotechnical earthquake engineering. Prentice-Hall; 1996.
[30] Beyer K, Bommer JJ. Relationships between median values and between aleatory variabilities for different definitions of the horizontal component of motion. Bull Seismol Soc Am 2006;96(4A):1512–22.
[31] Eurocode 2. Design of concrete structures. 1: general rule and rules for buildings. Brussels: ENV 1992-1-1; 1991.
[32] RAF-Structural Analysis and Design Software v. 3.3.2. Iraklion (Crete, Greece): TOL (Engineering Software House); 2012.
[33] Otani A. Inelastic analysis of RC frame structures. J Struct Div (ASCE) 1974;100(7):1433–49.
[34] Carr A. Ruaumoko – a program for inelastic time-history analysis, program manual. University of Canterbury, New Zealand: Department of Civil Engineering; 2004.
[35] Imbsen Software Systems. XTRACT: Version 3.0.5. Cross-sectional structural analysis of components. Sacramento (CA); 2006.
[36] Dimova SL, Negro P. Seismic assessment of an industrial frame structure designed according to Eurocodes. Part 2: capacity and vulnerability. Eng Struct 2005;27(5):24–735.
[37] Gunturi SKV, Shah HC. Building specific damage estimation. In: Proceedings of 10th world conference on earthquake engineering. Balkema, Madrid (Rotterdam); 1992. p. 6001–6.
[38] Naeim F, editor. The seismic design handbook. Boston, MA: Kluwer Academic; 2001.
[39] Park YJ, Ang AHS, Wen YK. Damage-limiting aseismic design of buildings. Earthq Spect 1987;3(1).
[40] Park YJ, Ang AHS. Mechanistic seismic damage model for reinforced-concrete. J. Struct. Eng – ASCE 1985;111(4):722–39.
[41] Kunnath SK, Reinhorn AM, Lobo RF. IDARC version 3: a program for the inelastic damage analysis of RC structures, Technical Report NCEER-92-0022. State University of New York (Buffalo, NY): National Centre for Earthquake Engineering Research; 1992.